arXiv:cond-mat/0406490v1 [cond-mat.mes-hall] 21 Jun 2004

Spin-Polarized Transport through Double Quantum Dots

Yoichi Tanaka and Norio Kawakami
Department of Applied Physics, Osaka University, Suita, Osaka 565-0871
(Dated: March 22, 2022)

We investigate spin-polarized transport phenomena through double quantum dots coupled to ferromagnetic leads in series. By means of the slave-boson mean-field approximation, we calculate the conductance in the Kondo regime for two different configurations of the leads: spin-polarization of two ferromagnetic leads is parallel or anti-parallel. It is found that transport shows some remarkable properties depending on the tunneling strength between two dots. These properties are explained in terms of the Kondo resonances in the local density of states.

PACS numbers:

I. INTRODUCTION

Since the Kondo effect was observed in a quantum dot system[1, 2], electron correlation effects in such nanoscale systems have attracted much attention. It was uncovered that the Kondo effect gives rise to remarkable properties in electron transport, which are not expected for free electron systems[3, 4, 5, 6, 7, 8]. For example, it makes tunneling transport possible at low temperatures even if the system is in the Coulomb blockade regime. Since the Kondo effect originates from many body effects due to internal spin degrees of freedom, transport properties are quite sensitive to applied magnetic fields[1, 2]. This fact has naturally stimulated intensive works on spin-dependent transport phenomena for a quantum dot connected to ferromagnetic leads [9, 10, 11, 12, 13, 14, 15, 16, 17], giving interesting examples in a rapidly developing field of magneto-electronics or spin-electronics[18, 19, 20, 21, 22].

When several quantum dots are connected to each other, they provide remarkable phenomena due to the interplay of electron correlations, interference effects, etc, which depend on how the dots are arranged: e.g. double quantum dots coupled in series or parallel[23, 24, 25, 26, 27, 28, 29, 30], T-shaped double dots[31, 32, 33], etc. In particular, the Kondo effect in double quantum dot systems has been observed experimentally[29, 30], opening prospects for exploring further exotic phenomena due to electron correlations in nanoscale systems.

In this paper, we study spin-dependent transport through a system of double quantum dots coupled to two ferromagnetic (FM) leads in series. Since the Kondo effect is sensitive to the presence of the FM leads, a variety of remarkable phenomena are expected to appear in transport at low temperatures. By applying the slave-boson mean-field approximation to the highly correlated Anderson model, we investigate the equilibrium and nonequilibrium transport with the use of Keldysh Green function techniques. We show that the strength of the inter-dot tunneling is an important key parameter to control transport phenomena via the modified Kondo resonances. We further discuss how the modified Kondo resonances affect transport properties for up- or down-spin electrons in the parallel and anti-parallel configurations of the FM leads.

The organization of this paper is as follows. In the next section, we describe the model and the method. Then in §3, we present the results for two different configurations: spin-polarization of two FM leads is parallel or anti-parallel. A brief summary is given in the last section.

II. MODEL AND METHOD

We consider spin-dependent transport properties of a system with double quantum dots coupled in series. In

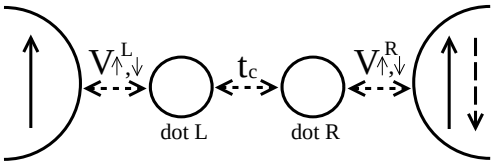


FIG. 1: Schematic picture of the double dot system coupled to the FM leads: t_c is the interdot coupling and $V_{\alpha\sigma}(\alpha = L, R, \sigma = \uparrow, \downarrow)$ represents the dot-lead tunneling for an electron with spin σ.

Fig.1 we schematically show our double-dot system. It is assumed that the left and right leads are spin-polarized, where the parallel (P) and anti-parallel (AP) configurations are considered. In the following discussions, the intradot Coulomb interaction U is sufficiently large, so that double occupancy at each dot is forbidden, which allows us to use slave-boson representation[34, 35] of correlated electrons in the dots. In terms of this representation, we can model the system in Fig.1 with a $N(=2)$ fold degenerate Anderson Hamiltonian including an additional

term for interdot coupling,

$$\begin{aligned} H &= \sum_{k_\alpha,\sigma} \varepsilon_{k_\alpha\sigma} c^\dagger_{k_\alpha\sigma} c_{k_\alpha\sigma} + \sum_{\alpha,\sigma} \varepsilon_{\alpha\sigma} f^\dagger_{\alpha\sigma} f_{\alpha\sigma} \\ &+ \frac{t_c}{N} \sum_\sigma (f^\dagger_{L\sigma} b_L b^\dagger_R f_{R\sigma} + f^\dagger_{R\sigma} b_R b^\dagger_L f_{L\sigma}) \\ &+ \frac{1}{\sqrt{N}} \sum_{k_\alpha,\sigma} V_{\alpha\sigma} (c^\dagger_{k_\alpha\sigma} b^\dagger_\alpha f_{\alpha\sigma} + f^\dagger_{\alpha\sigma} b_\alpha c_{k_\alpha\sigma}) \\ &+ \sum_\alpha \lambda_\alpha (\sum_\sigma f^\dagger_{\alpha\sigma} f_{\alpha\sigma} + b^\dagger_\alpha b_\alpha - 1), \end{aligned} \tag{1}$$

where $c^\dagger_{k_\alpha\sigma}(c_{k_\alpha\sigma})$ is the creation (annihilation) operator for an electron with spin σ in the lead α ($\alpha = L, R$). According to the slave-boson representation, the creation (annihilation) operator of electrons in the left or right dot, $d^\dagger_{\alpha\sigma}(d_{\alpha\sigma})$, is replaced by $d^\dagger_{\alpha\sigma} \to f^\dagger_{\alpha\sigma} b_\alpha$ ($d_{\alpha\sigma} \to f_{\alpha\sigma} b^\dagger_\alpha$), where b_α ($f_{\alpha\sigma}$) is the slave-boson (pseudo-fermion) annihilation operator for an empty state (singly occupied state). The last term with the Lagrange multiplier λ_α is introduced so as to incorporate the constraint imposed on the slave particles, $\sum_{\sigma=\uparrow,\downarrow} f^\dagger_{\alpha\sigma} f_{\alpha\sigma} + b^\dagger_\alpha b_\alpha = 1$. For simplicity, we consider the symmetric dots with $\varepsilon_{L\sigma} = \varepsilon_{R\sigma} = \varepsilon_0$. The mixing term $V_{\alpha\sigma}$ in (1) leads to the linewidth function

$$\Gamma^\alpha_\sigma(\varepsilon) = \pi \sum_{k_\alpha,\sigma} |V_{\alpha,\sigma}|^2 \delta(\varepsilon - \varepsilon_{k_\alpha\sigma}), \tag{2}$$

which is reduced to an energy-independent constant Γ^α_σ in the wide band limit. Here, we introduce the effective spin-polarization strength p, following the definition given in the literature: [10, 11, 12, 15, 16]

$$p = \frac{\Gamma^\alpha_\sigma - \Gamma^\alpha_{\bar\sigma}}{\Gamma^\alpha_\sigma + \Gamma^\alpha_{\bar\sigma}} \ (0 \le p \le 1). \tag{3}$$

This quantity is convenient to represent how large the strength of the spin polarization is. From the definition of p, Γ^α_σ is expressed in the case of the P and AP configurations,

$$\mathrm{P} : \Gamma^L_\uparrow = \Gamma^R_\uparrow = (1+p)\Gamma_0 \,,\ \Gamma^L_\downarrow = \Gamma^R_\downarrow = (1-p)\Gamma_0 \tag{4}$$

$$\mathrm{AP} : \Gamma^L_\uparrow = \Gamma^R_\downarrow = (1+p)\Gamma_0 \,,\ \Gamma^L_\downarrow = \Gamma^R_\uparrow = (1-p)\Gamma_0, \tag{5}$$

where Γ_0 is the value at $p = 0$.

To analyze our model, we use the slave-boson mean-field approximation [25, 27, 28, 34, 35], in which boson fields are approximated by their mean values, $b_\alpha(t)/\sqrt{N} \to \langle b_\alpha(t)\rangle/\sqrt{N} = \tilde b_\alpha$. By introducing the renormalized quantities $\tilde V_{\alpha\sigma} = V_{\alpha\sigma}\tilde b_\alpha$, $\tilde t_c = t_c \tilde b_L \tilde b_R$, and $\tilde\varepsilon_\alpha = \varepsilon_0 + \lambda_\alpha$, the total Hamiltonian (1) is now replaced by

$$\begin{aligned} \tilde H &= \sum_{k_\alpha,\sigma} \varepsilon_{k_\alpha\sigma} c^\dagger_{k_\alpha\sigma} c_{k_\alpha\sigma} + \sum_{\alpha,\sigma} \tilde\varepsilon_\alpha f^\dagger_{\alpha\sigma} f_{\alpha\sigma} \\ &+ \tilde t_c \sum_\sigma (f^\dagger_{L\sigma} f_{R\sigma} + f^\dagger_{R\sigma} f_{L\sigma}) \\ &+ \sum_{k_\alpha,\sigma} \tilde V_{\alpha\sigma} (c^\dagger_{k_\alpha\sigma} f_{\alpha\sigma} + f^\dagger_{\alpha\sigma} c_{k_\alpha\sigma}) \\ &+ \sum_\alpha \lambda_\alpha (N\tilde b^2_\alpha - 1). \end{aligned} \tag{6}$$

To determine the mean-field values of $(\tilde b_L, \tilde b_R, \lambda_L, \lambda_R)$, we employ the equation of motion method with the non-equilibrium Keldysh Green functions. This gives the following set of self-consistent equations,

$$\tilde b^2_{L(R)} - i \sum_\sigma \int \frac{d\varepsilon}{4\pi} G^<_{L,L(R,R)\sigma}(\varepsilon) = \frac{1}{2}, \tag{7}$$

$$(\tilde\varepsilon_{L(R)} - \varepsilon_0)\tilde b^2_{L(R)} - i \sum_\sigma \int \frac{d\varepsilon}{4\pi} (\varepsilon - \tilde\varepsilon_{L(R)})\, G^<_{L,L(R,R)\sigma}(\varepsilon) = 0, \tag{8}$$

where $G^<_{L,L(R,R)\sigma}(\varepsilon)$ is the Fourier transform of the Keldysh Green function $G^<_{\alpha,\alpha'\sigma}(t-t') \equiv i\langle f^\dagger_{\alpha'\sigma}(t') f_{\alpha\sigma}(t)\rangle$. The first equation represents the constraint imposed on the slave particles, while the second one is obtained from the stationary condition that the boson field is time-independent at the mean-field level. From the equation of motion of the operator $f_{\alpha\sigma}$ [25, 36], we have the explicit form of the Green function,

$$G^<_{L,L(R,R)\sigma}(\varepsilon) = \frac{2i\left\{ f_{L(R)}(\varepsilon)\tilde\Gamma^{L(R)}_\sigma \left[(\varepsilon - \tilde\varepsilon_{R(L)})^2 + (\tilde\Gamma^{R(L)}_\sigma)^2\right] + f_{R(L)}(\varepsilon)\tilde\Gamma^{R(L)}_\sigma \tilde t_c{}^2 \right\}}{\left| (\varepsilon - \tilde\varepsilon_L + i\tilde\Gamma^L_\sigma)(\varepsilon - \tilde\varepsilon_R + i\tilde\Gamma^R_\sigma) - \tilde t_c{}^2 \right|^2} \tag{9}$$

with $\tilde\Gamma^\alpha_\sigma = \tilde b^2_\alpha \Gamma^\alpha_\sigma\, (\alpha = L, R)$. Note here that we have derived the above formulae by applying the analytic continuation rules to the equation of motion of the time-ordered Green functions along a complex contour.

By using the renormalized parameters determined self-consistently, we obtain the current I through the two

dots, [23, 25, 27, 36]

$$I = \frac{2e\Gamma_0}{h} \sum_\sigma \int d\varepsilon \, (f_L(\varepsilon) - f_R(\varepsilon)) \, T_\sigma(\varepsilon) \qquad (10)$$

with the Fermi function $f_\alpha(\varepsilon)$, where the transmission probability $T_\sigma(\varepsilon)$ for spin σ is

$$T_\sigma(\varepsilon) = \frac{2\tilde{t_c}^2 \tilde{\Gamma}_\sigma^L \tilde{\Gamma}_\sigma^R}{\left| (\varepsilon - \tilde{\varepsilon}_L + i\tilde{\Gamma}_\sigma^L)(\varepsilon - \tilde{\varepsilon}_R + i\tilde{\Gamma}_\sigma^R) - \tilde{t_c}^2 \right|^2} \, . \quad (11)$$

We can thus compute the differential conductance $G = dI/dV$ from the current I in (10). Moreover, we obtain the density of states (DOS) for the dot α ($\alpha = L$ or R) as

$$\rho_{\alpha,\sigma}(\varepsilon) = -\frac{1}{\pi} \tilde{b}_\alpha^2 \mathrm{Im} G^r_{\alpha,\alpha\sigma}(\varepsilon), \qquad (12)$$

where $G^r_{\alpha,\alpha\sigma}(\varepsilon)$ is the Fourier transform of the Keldysh Green function $G^r_{\alpha,\alpha\sigma}(t - t') \equiv -i\theta(t - t')\langle\{f_{\alpha\sigma}(t), f^\dagger_{\alpha\sigma}(t')\}\rangle$, which is given by

$$G^r_{L,L(R,R)\sigma}(\varepsilon) = \frac{(\varepsilon - \tilde{\varepsilon}_{R(L)} + i\tilde{\Gamma}_\sigma^{R(L)})}{(\varepsilon - \tilde{\varepsilon}_L + i\tilde{\Gamma}_\sigma^L)(\varepsilon - \tilde{\varepsilon}_R + i\tilde{\Gamma}_\sigma^R) - \tilde{t_c}^2} . \qquad (13)$$

This completes our formulation of the non-equilibrium transport for the double-dot system with spin polarization.

III. NUMERICAL RESULTS

In this section, we discuss the results computed at absolute zero for the P and AP configurations separately. For simplicity, the band width of the leads is taken as $D = 60\Gamma_0$ and the bare level for two dots is fixed as $\varepsilon_0 = -3.5\Gamma_0$ (Kondo regime). We will use Γ_0 as the unit of the energy and choose the Fermi level at $V = 0$ as the origin of the energy.

A. Parallel configuration

Let us start our discussions with the parallel (P) configuration of the polarized leads.

1. *Equilibrium case* ($V = 0$)

We first investigate transport properties of the equilibrium dot system where the bias voltage V is infinitesimally small. In Fig. 2, we plot the linear conductance $G_{V=0} = dI/dV|_{V=0}$ as a function of the spin polarization strength p for various interdot couplings. For $t_c = 0.3$, $G_{V=0}$ exhibits a maximum around $p = 0.7$, whereas it decreases monotonically for $t_c = 1.0$ and 1.5. To clearly observe the characteristic p-dependence in the conductance,

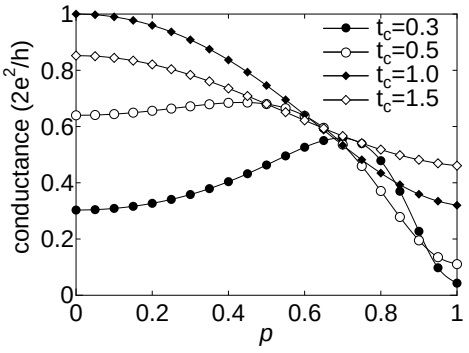


FIG. 2: Linear conductance $G_{V=0} = dI/dV|_{V=0}$ as a function of the spin-polarization strength p for $t_c = 0.3, 0.5, 1.0$ and 1.5.

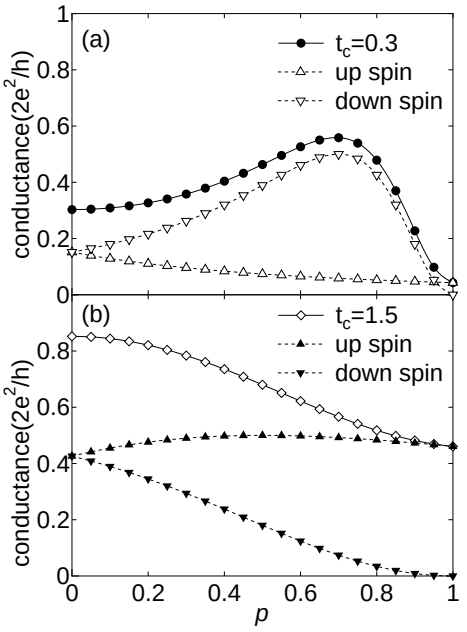


FIG. 3: The contribution of up and down spin electrons to the conductance for (a) $t_c = 0.3$ and (b) 1.5.

let us consider the contribution of up- and down-spin electrons to $G_{V=0}$. For small interdot coupling ($t_c = 0.3$) in Fig. 3(a), it is seen that down-spin (i.e. minority-spin) electrons contribute dominantly to $G_{V=0}$ at large p, featuring a maximum structure around $p = 0.7$. However, for larger interdot couplings (e.g. $t_c = 1.5$) in Fig. 3(b), $G_{V=0}$ gets dominated by up-spin (i.e. majority-spin) electrons as p increases.

The origin of the above characteristic properties can be seen in the formation of the modified Kondo resonances in the presence of p. Figures 4 and 5 show the local DOS for up- and down-spin electrons of the dots around the Fermi energy $\varepsilon = 0$. In the equilibrium case with $V = 0$, we denote the DOS for the left and right dots as $\rho_\sigma(\varepsilon) = \rho_{L\sigma}(\varepsilon) = \rho_{R\sigma}(\varepsilon)$.

In the absence of p, one can see the formation of the

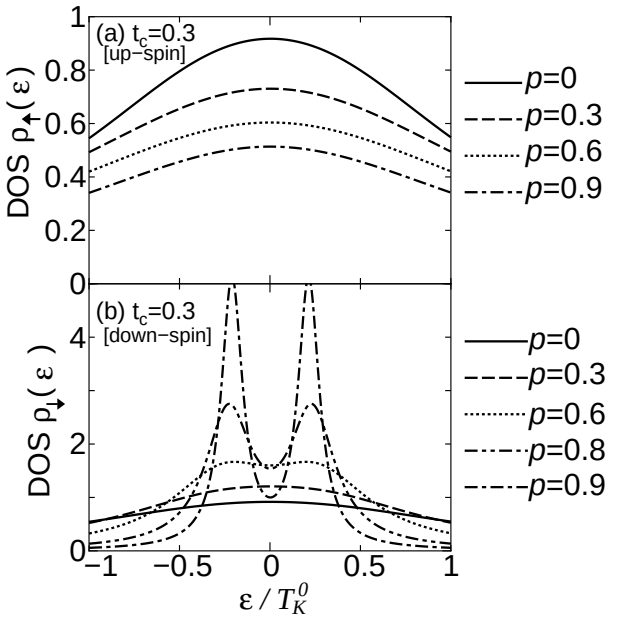


FIG. 4: DOS for (a) up- and (b) down-spin electrons of the dots in the case of $t_c = 0.3$. The energy ε is normalized by the Kondo temperature in the equilibrium case T_K^0 ($T_K^0 \simeq 10^{-3}\Gamma_0$).

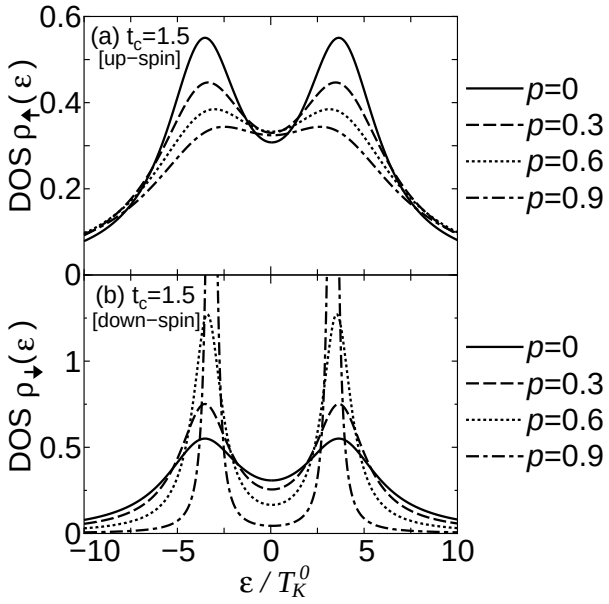


FIG. 5: DOS of the dots for (a) up- and (b) down-spin electrons in the case of $t_c = 1.5$.

Kondo resonance around $\varepsilon = 0$, which is renormalized about 10^{-3} smaller than the bare resonance. First we consider the case of $t_c = 0.3$. As the bare resonance width for up-spin electrons increases with the increase of p, according to Eq.(4), the resulting Kondo resonance for $\rho_\uparrow(\varepsilon)$ in Fig. 4(a) becomes broad, so that $\rho_\uparrow(0)$, which determines $G_{V=0}$, decreases. On the other hand, as seen from $\rho_\downarrow(\varepsilon)$ in Fig. 4(b), the width of the Kondo resonance for down spin electrons becomes smaller with increasing p. Therefore, the corresponding peak in $\rho_\downarrow(\varepsilon)$ splits into two sub-peaks when its width gets comparable to the renormalized interdot coupling $\tilde{t}_c$. Namely, the Kondo resonances in the left and right dots are combined into the bonding and antibonding Kondo resonances, which are respectively located around

$$\varepsilon_\pm = \frac{1}{2}\left\{(\tilde{\varepsilon}_L + \tilde{\varepsilon}_R) \pm \sqrt{(\tilde{\varepsilon}_L - \tilde{\varepsilon}_R)^2 + 4\tilde{t_c}^2}\right\}. \qquad (14)$$

Since $\tilde{\varepsilon}_L = \tilde{\varepsilon}_R$ at $V = 0$, the energy difference $2\tilde{t_c}(= \varepsilon_+ - \varepsilon_-)$ gives the splitting of the Kondo resonances. Thus, $\rho_\downarrow(0)$ increases first and then decreases with the increase of p. The above p-dependence of the Kondo resonances naturally explains the characteristic behavior of $G_{V=0}$ in Fig. 3(a).

We next discuss the case of $t_c = 1.5$. As seen in Fig. 5, the large interdot coupling causes the splitting of the Kondo resonances even at $p = 0$, which is obscured (sharpened) for up spins (down spins) with the increase of p. As a result, $\rho_\uparrow(0)$ little changes, while $\rho_\downarrow(0)$ monotonically decreases as p increases. This clarifies why the contribution of up-spin electrons to $G_{V=0}$ is almost independent of p whereas that of down spin electrons decreases with increasing p in Fig. 3(b).

When we change the strength of tunneling t_c, the system changes gradually between the above two typical cases.

2. *Nonequilibrium case* ($V \neq 0$)

We next show the results in the nonequilibrium case. By using Eq.(10), we calculate the current I through the system as a function of V: we set the chemical potentials $\mu_L = V/2$ and $\mu_R = -V/2$. We wish to mention here that Aguado et al. studied transport properties for normal leads with finite bias voltage.[25]

Figure 6 shows the I-V characteristics as well as the contribution of up- and down-spin electrons. Note that the conductance $G_{V=0}$ discussed above coincides with the gradient of the I-V curves at $V = 0$ in Fig. 6. For $t_c = 0.3$, as shown in Fig. 6(a), the current once increases and then decreases after making a peak structure in its V dependence. The peak structure becomes sharp with the increase of p, which is mainly caused by down-spin electrons, as seen in Fig. 6(b). We can thus see that for finite p the current is dominated by down spin electrons for small V, while it is mainly contributed by up-spin electrons for large V. In contrast, we encounter different behavior for $t_c = 1.5$ in Figs. 6(c) and (d). In the voltage regime shown in the figure, the current I is almost linear in V, and is dominated by up-spin electrons as p increases.

As in the equilibrium case, we interpret the above I-V characteristics in terms of the modified Kondo reso-

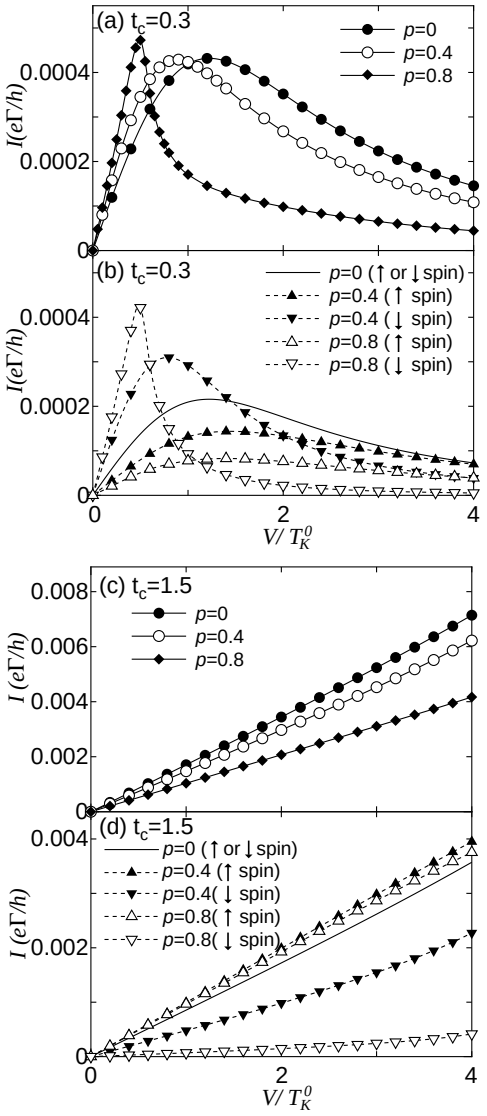


FIG. 6: (a) I-V characteristics and (b) the contribution of up- and down-spin electrons for $t_c = 0.3$. Similar plots are shown in (c) and (d) for $t_c = 1.5$.

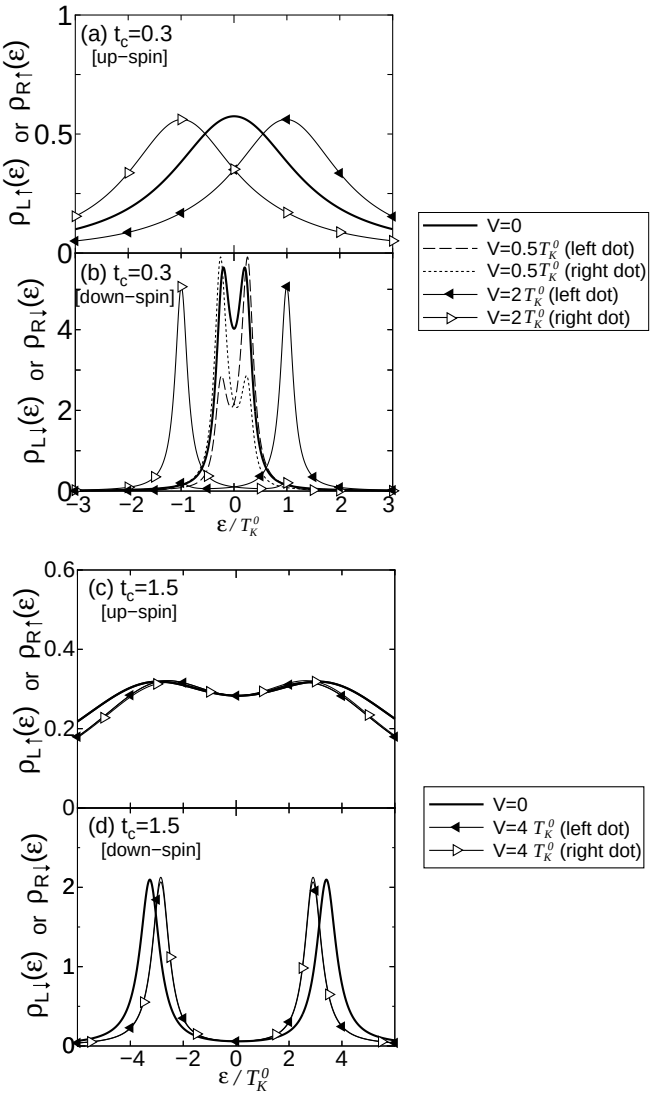


FIG. 7: DOS for left and right dots at $p = 0.8$ in the nonequilibrium case: $t_c = 0.3$ for (a) up- and (b) down-spin electrons; $t_c = 1.5$ for (c) up- and (d) down-spin electrons.

nances. In Fig. 7 we show the Kondo resonances in the nonequilibrium case by exploiting $t_c = 0.3$ and $t_c = 1.5$ with a typical spin-polarization $p = 0.8$.

Let us first look at the Kondo resonance at $t_c = 0.3$ in Figs. 7(a) and (b). At $V = 0$, the DOS for up-spin electrons shows a broad hump, while that for down-spin electrons has sharp peaks with small splitting due to t_c. With increasing V, the Kondo resonance of the left (right) dot is shifted, following change in the chemical potential of the left (right) lead. Roughly speaking, the current I depends on the overlap of these two Kondo resonances in the energy region between μ_L and μ_R ($-V/2 < \varepsilon < V/2$ in Fig. 7). By this reason, at small V, the current I for up-spin electrons gradually increases with the increase of V and goes down reflecting the decrease in the overlap of the Kondo resonances for larger V. On the other hand, for down spins (Fig. 7(b)), the splitting of the resonances is enlarged as V increases, leading to the well-separated peaks. Correspondingly, the current I rises sharply for small V, and then goes down quickly as V gets large.

When the inter-dot coupling is large ($t_c = 1.5$), we can see the splitting of the Kondo resonances both for up-spin and down-spin electrons at $V = 0$, although they are well separated (Fig. 7(d)) for down spins but more or less obscured for up spins (Fig. 7(c)). A remarkable point is that their shapes little change with increasing V, because the coupling between the two dots is much larger than the applied bias. Note that the DOS for up- and down-spin electrons is almost flat in the vicinity of the Fermi energy, so that the current I is approximately linear in the bias voltage and mainly caused by up-spin electrons, in accordance with the results of Figs. 6(c) and (d). Here, we wish to mention what happens for larger

voltage in the case of $t_c = 1.5$. We have checked that the system undergoes a first-order phase transition when V further increases beyond $V/T_K \sim 4$, where the current drops discontinuously. This implies that a strongly coupled molecule is formed between two dots, which is almost decoupled from two leads. Such a phenomenon was already pointed out in the $p = 0$ case.[25] The detail of the first-order transition can be found there.

B. Antiparallel configuration

We now move to the system with the AP configuration of the polarized leads. We can continue discussions similarly to the above P case, so that we summarize the essential points briefly.

1. *Equilibrium case* ($V = 0$)

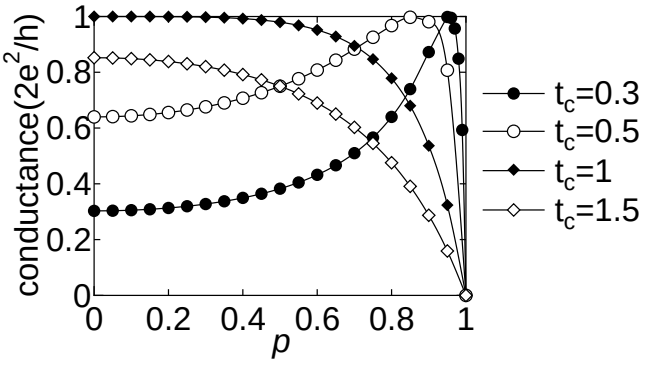


FIG. 8: Linear conductance $G_{V=0}$ as a function of the spin polarization strength p for the AP configuration.

We start with the equilibrium case. In Fig. 8, we plot the linear conductance $G_{V=0}$ as a function of the spin polarization strength p. Note that the contribution of up- and down-spin electrons to the total conductance is same in the AP case. Nevertheless, we observe the behavior somewhat analogous to the case of the P configuration: for small t_c the total conductance features a peak structure in its p dependence, while it decreases monotonically for large t_c. On the other hand, for the fully polarized case with $p = 1$, the current vanishes in the present case in contrast to the P configuration.

Similarly to the P case, the characteristics in the conductance can be interpreted in terms of the modified Kondo resonances. In Fig. 9 we show the local DOS. According to Eq.(5), we see that $\rho_{L\uparrow}(\varepsilon)$ ($\rho_{L\downarrow}(\varepsilon)$) is identical to $\rho_{R\downarrow}(\varepsilon)$ ($\rho_{R\uparrow}(\varepsilon)$). We focus on the up-spin electrons for simplicity. $\rho_{R\uparrow}(\varepsilon)$ and $\rho_{L\uparrow}(\varepsilon)$ are mixed with each other in the presence of the coupling t_c. We note that the right (left) resonance gets narrower (broader) with the increase of p, so that for $t_c = 0.3$ there appears a dip structure in $\rho_{L\uparrow}(\varepsilon)$ around $\varepsilon = 0$, while a single peak structure

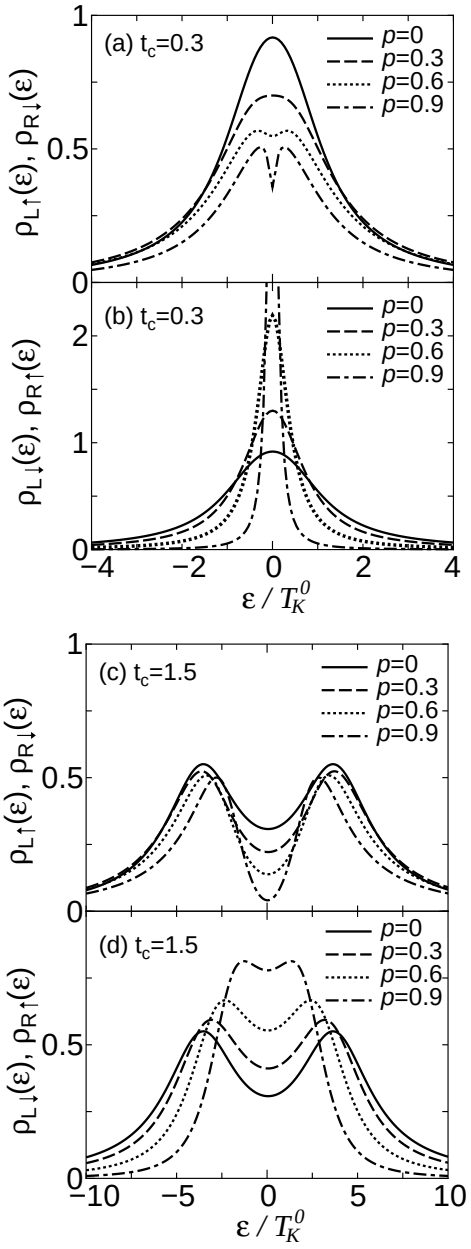


FIG. 9: DOS of the left and right dots at various p: $t_c = 0.3$ in (a) and (b); $t_c = 1.5$ in (c) and (d).

still remains in $\rho_{R\uparrow}(\varepsilon)$, as seen from Figs. 9(a) and (b). Recall that the conductance is roughly given by the product of $\rho_{R\uparrow}(\varepsilon)$ and $\rho_{L\uparrow}(\varepsilon)$ at the Fermi level. Therefore, we naturally see that the combination of the peak and dip structures in the DOS gives a maximum structure in the conductance for $t_c = 0.3$. On the other hand, for $t_c = 1.5$, the development of the peak structure in $\rho_{R\uparrow}(\varepsilon)$ is slow with the increase of p. Thus the development of the dip structure in $\rho_{L\uparrow}(\varepsilon)$ dominates the slight change in $\rho_{R\uparrow}(\varepsilon)$, leading to the monotonic decrease of the conductance as a function of p, as seen in Fig. 8. Note that at $p = 1$, the current vanishes, in contrast to the P con-

figuration, because either of the DOS of the right or left dot vanishes at the Fermi level.

2. *Nonequilibrium systems* ($V \neq 0$)

We finally show the results in the nonequilibrium case with the AP configuration. Figure 10 shows the I-V characteristics of $t_c = 0.3$ and 1.5 for various choices of p. We note again that the V-dependence of the total current shows similar behavior to that for the P configuration (Fig. 6) although the origin of the characteristics is somewhat different, as mentioned above. Shown in Fig. 11 are the Kondo resonances in nonequilibrium case at $p = 0.6$. When the bias voltage is applied, the peak position of $\rho_{L\sigma}(\varepsilon)$, $\rho_{R\sigma}(\varepsilon)$ ($\sigma = \uparrow$ or $\downarrow$) follows the change of the left or right chemical potential, as shown in Figs. 11(a) and (b). As mentioned above, the current for up- or down-spin electrons is controlled by the overlap of the Kondo resonances of the left and right dots in the region of $\varepsilon = -V/2$ to $\varepsilon = V/2$ in Fig. 11. This gives rise to the maximum structure in the I-V characteristics for $t_c = 0.3$. As seen in Figs. 11(c) and (d) for $t_c = 1.5$, the shape of the Kondo resonances with splitting is not altered so much up to a certain voltage, giving a linear conductance, as is the case for the P configuration. For larger voltage, the system suffers from a sudden phase transition accompanied by discontinuous drop in I [25].

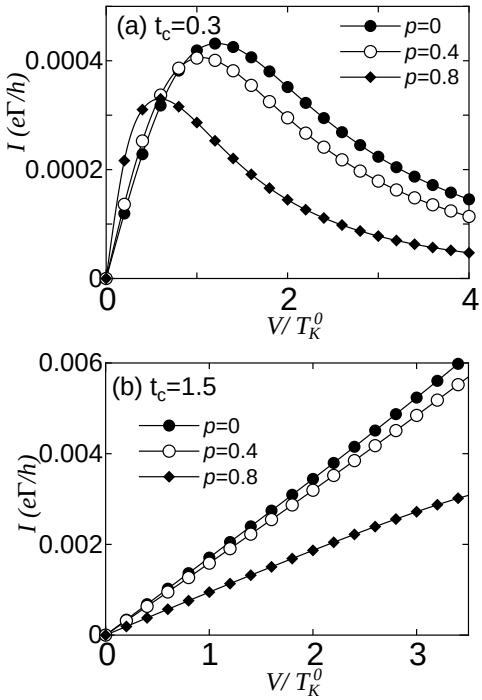


FIG. 10: I-V characteristics for the AP configuration at $p = 0, 0.4$ and 0.8: (a)$t_c = 0.3$ and (b)$t_c = 1.5$.

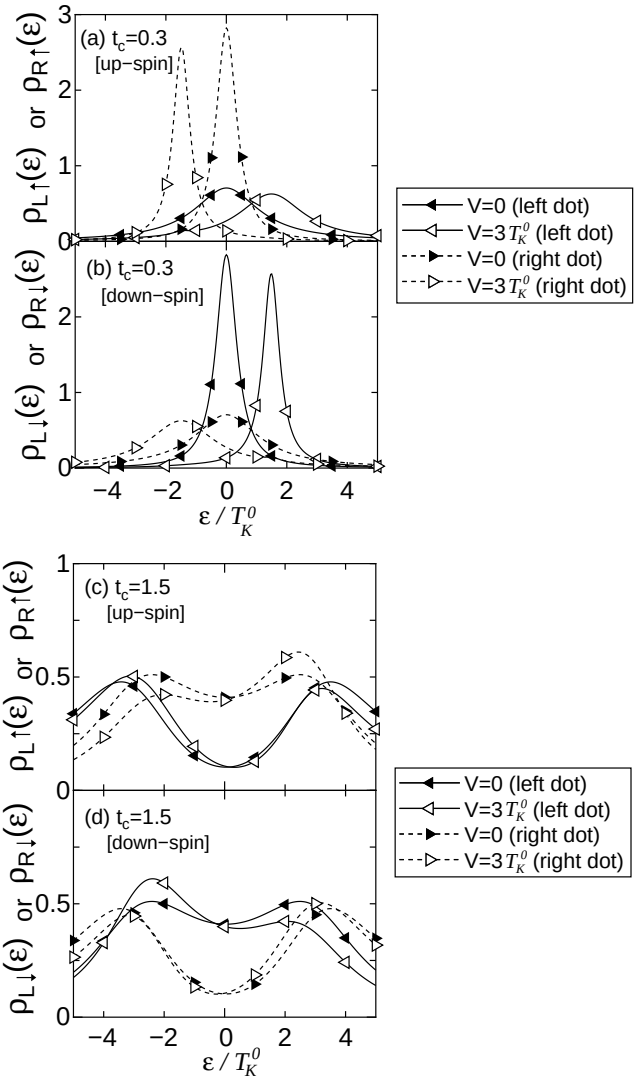


FIG. 11: DOS of the left dot (solid line) and right dot (broken line) for the bias voltage $V = 0$ and $3T_K^0$ at $p = 0.6$: (a) up- and (b) down-spin electrons in the case of $t_c = 0.3$; (c) up- and (d) down-spin electrons in the case of $t_c = 1.5$.

IV. SUMMARY

We have discussed equilibrium and non-equilibrium transport properties of double quantum dots attached to the FM leads in series. It has been found that, under the influence of the FM leads, transport shows the characteristic properties due to the modified Kondo resonances. We have clarified that the total conductance shows analogous p-dependence between P and AP configurations of the leads, although the origin of such behavior is somewhat different from each other.

For the P configuration, at small inter-dot coupling t_c, the conductance of down-spin (minority spin) electrons dominates that of up-spin (majority spin) electrons, giving rise to a peak structure in the p-dependent conductance. On the other hand, for large coupling t_c,

the conductance exhibits monotonic p-dependence, and is mainly contributed by up-spin electrons in the large p region. For the AP configuration, we have observed similar p-dependence in the total conductance, although the contribution of the up- or down-spin electrons is always same in this case.

We have also studied the current I at finite bias voltage, which again shows distinct properties depending on t_c. For small inter-dot coupling, the Kondo resonances of the left and right dots are shifted, following the change in the chemical potential. This gives rise to a characteristic peak structure in the V dependence of the current. On the other hand, for large inter-dot coupling, the shape of the modified Kondo resonances is not changed so much up to large V, leading to the linear conductance in the wide V region, beyond which the systems undergoes a first-order transition accompanied by the sudden decrease of the current.

Experimentally, the Kondo effect in double dot systems has been observed recently[29, 30]. We thus expect that in the near future, it may become possible to observe the Kondo effect in double dot systems coupled to the FM leads, providing further interesting examples of correlation effects in the context of spin-dependent transport in nanoscale systems.

Acknowledgments

The work is partly supported by a Grant-in-Aid from the Ministry of Education, Culture, Sports, Science and Technology of Japan.

[1] D. Goldhaber-Gordon, H. Shtrikman, D. Mahalu, D. Abusch-Magder, U. Meirav and M. A. Kanster: Nature **391** (1998) 156 ; D. Goldhaber-Golden, J. Göres, M. A. Kastner, H. Shtrikman, D. Mahalu and U. Meirav: Phys. Rev. Lett. **81** (1998) 5225.

[2] S. M. Cronenwett, T. H. Oosterkamp and L. P. Kouwenhoven: Science **281** (1998) 540.

[3] T. K. Ng and P. A. Lee: Phys. Rev. Lett. **61** (1988) 1768.

[4] L. I. Glazman and M. E. Raikh: JETP Lett. **47** (1988) 452.

[5] A. Kawabata: J. Phys. Soc. Jpn. **60** (1991) 3222.

[6] Y. Meir and N. S. Wingreen: Phys. Rev. Lett. **68** (1992) 2512; Y. Meir, N. S. Wingreen and P. A. Lee: Phys. Rev. Lett. **70** (1993) 2601; A. -P. Jauho, N. S. Wingreen and Y. Meir: Phys. Rev. B **50** (1994) 5528.

[7] A. Oguri, H. Ishii and T. Saso: Phys. Rev. B **51** (1995) 4715.

[8] W. Izumida, O. Sakai and Y. Shimizu: J. Phys. Soc. Jpn. **67** (1998) 2444.

[9] B. Wang, J. Wang and H. Guo: J. Phys. Soc. Jpn. **70** (2001) 2645.

[10] P. Zhang, Q. -K. Xue, Y. Wang and X. C. Xie: Phys. Rev. Lett. **89** (2002) 286803.

[11] N. Sergueev, Q. -f. Sun, H. Guo, B. G. Wang and J. Wang: Phys. Rev. B **65** (2002) 165303.

[12] J. Ma, B. Dong and X. L. Lei: cond-mat/0212645.

[13] R. López and D. Sánchez: Phys. Rev. Lett. **90** (2003) 116602.

[14] J. König and J. Martinek: Phys. Rev. Lett. **90** (2003) 166602.

[15] J. Martinek, Y. Utsumi, H. Imamura, J. Barnaś, S. Maekawa, J. König and G. Schön: Phys. Rev. Lett. **91** (2003) 127203.

[16] B. Dong, H. L. Cui, S. Y. Liu and X. L. Lei: cond-mat/0302372.

[17] M. -S. Choi, D. Sánchez and R. López: Phys. Rev. Lett. **92** (2004) 056601.

[18] M. Julliere: Phys. Lett. **54A** (1975) 225.

[19] M. N. Baibich, J. M. Broto, A. Fert, F. Nguyen Van Dau, F. Petroff, P. Eitenne, G. Creuzet, A. Friederich and J. Chazelas: Phys. Rev. Lett. **61** (1988) 2472.

[20] J. C. Slonczewski: Phys. Rev. B **39** (1989) 6995.

[21] G. A. Prinz: Science **282** (1998) 1660.

[22] S. A. Wolf, D. D. Awschalom, R. A. Buhrman, J. M. Daughton, S. von Molnár, M. L. Roukes, A. Y. Chtchelkanova and D. M. Treger: Science **294** (2001) 1488.

[23] T. Aono, M. Eto and K. Kawamura: J. Phys. Soc. Jpn. **67** (1998) 1860.

[24] A. Georges and Y. Meir: Phys. Rev. Lett. **82** (1999) 3508.

[25] R. Aguado and D. C. Langreth: Phys. Rev. Lett. **85** (2000) 1946.

[26] W. Izumida and O. Sakai: Phys. Rev. B **62** (2000) 10260.

[27] T. Aono and M. Eto: Phys. Rev. B **63** (2001) 125327.

[28] R. López R. Aguado and G. Platero: Phys. Rev. Lett. **89** (2002) 136802.

[29] H. Jeong, A. M. Chang and M. R. Melloch: Science **293** (2001) 2221.

[30] J. C. Chen, A. M. Chang and M. R. Melloch: Phys. Rev. Lett. **92** (2004) 176801.

[31] T. -S. Kim and S. Hershfield: Phys. Rev. B **63** (2001) 245326.

[32] K. Kikoin and Y. Avishai: Phys. Rev. Lett. **86** (2001) 2090; K. Kikoin and Y. Avishai: Phys. Rev. B **65** (2002) 115329.

[33] Y. Takazawa, Y. Imai and N. Kawakami: J. Phys. Soc. Jpn. **71** (2002) 2234.

[34] A. C. Hewson: *The Kondo Problem to Heavy Fermions* (Cambridge University Press, Cambridge, 1993).

[35] P. Coleman: Phys. Rev. B **29** (1984) 3035.

[36] H. Haug and A. -P. Jauho: *Quantum Kinetics in Transport and Optics of Semi-conductors*, edited by M. Cardona et al. (Springer-Verlag, 1998).